THE JOURNAL OF PHYSICAL CHEMISTRY B

Article

pubs.acs.org/JPCB

Neutral Carotenoid Radicals in Photoprotection of Wild-Type *Arabidopsis thaliana*

Adam Magyar,[†] Michael K. Bowman,[†] Péter Molnár,[‡] and L. Kispert*[,†]

[†]Department of Chemistry, The University of Alabama, Box 870336, Tuscaloosa, Alabama 35487-0336, United States

[‡]Department of Pharmacognosy, University of Pécs, Medical School, H-7624 Pécs, Rókus u. 2, Pécs, Hungary

Supporting Information

ABSTRACT: The deprotonation of naturally occurring zeaxanthin (Zea) radical cations ($Zea^{\bullet+}$) to form neutral radicals (#$Zea^{\bullet}$) and their involvement in the qE portion of nonphotochemical quenching (NPQ) was examined. The radical cations are weak acids, and readily deprotonate to a long-lived neutral radical (#$Zea^{\bullet}$) that could serve as long-lived quenching sites. When #$Zea^{\bullet}$ is eventually neutralized and Zea is reformed in the presence of D_2O, the Zea has an opportunity to undergo H/D exchange. This paper examines evidence for H/D exchange specific to qE activity in *Arabidopsis thaliana*. We demonstrate that $Zea^{\bullet+}$ formed chemically via oxidation of Zea by Fe(III) in the presence of D_2O undergoes H/D exchange with a significant intensity increase of the M+1 (d_1Zea) and M+2 (d_2Zea) mass peaks in the mass spectrum. Then leaves from wild-type *A. thaliana* were infiltrated with either D_2O or H_2O and exposed to light. The carotenoids were extracted and analyzed via electrospray ionization liquid chromatography/mass spectrometry (LC/MS) to examine the mass peak distribution of Zea. Only leaves exposed to light intensity that triggers qE in *A. thaliana* (>300 μE $m^{-2}s^{-1}$) showed H/D exchange. This result suggests that #$Zea^{\bullet}$ can form by the deprotonation of the weak acid $Zea^{\bullet+}$ during qE, and its possible impact on qE must be considered.

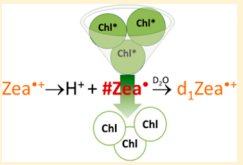

INTRODUCTION

Plants use photosynthesis to generate carbohydrates and oxygen from CO_2 and water. Light energy is necessary for this process, but excessive light is harmful to the plant. Chlorophyll (Chl) absorbs light and is transformed into its excited state. When light is absorbed at a higher rate than the photosynthetic enzymes can process, that energy must be dissipated in the form of heat or fluorescence in order to prevent unwanted reactions of the excited state Chl, which can generate singlet oxygen, damage proteins, and bleach chlorophyll in a variety of photochemical reactions detrimental to the plant.[1−3] Controlled dissipation of the excess energy as heat is very important for the plant.[4,5] Previous studies[6] have pointed out that the favorable formation of carotenoid neutral radicals at the terminal end groups for zeaxanthin (Zea) and lutein (Lut) radical cations correlates with their ability to quench excess energy in addition to their role as antennae. However, neutral radicals do not form at the terminal end groups of carotenoid radical cations that are not involved in quenching such as violaxanthin (Viol) and 9-*cis*-neoxanthin.[6]

Plants have several redundant mechanisms for protection from excess light, collectively known as nonphotochemical quenching (NPQ).[7−10] One important form of NPQ is qE, which is characterized by a decrease in fluorescence. *A. thaliana* mutants show a strong connection between Zea[11] and the qE component of NPQ. Femtosecond transient absorption spectroscopy detects a charge transfer complex between Zea and Chl in light-harvesting complex proteins CP24, CP26, and CP29 in qE proficient plants.[12,13] Excited Chl generated in these proteins are quenched by formation of a charge transfer complex with Zea, producing[12,13] a radical cation of Zea and a Chl radical anion: Zea + Chl + $h\nu$ → $Zea^{\bullet+}\cdots Chl^{\bullet-}$.

At low light levels, the photosynthetic apparatus needs every light photon available, and qE becomes detrimental to the plant. So at low light, Zea is converted into Viol, which does not support qE. The light-intensity-dependent interconversion of Zea and Viol is known as the xanthophyll cycle (Scheme 1). Zea is formed from Viol by violaxanthin de-epoxidase (VDE), which is triggered by excess protons and low pH.[14] The epoxide groups of Viol are removed by VDE to form Zea. At low light, VDE is no longer activated, and Zea is epoxidized by zeaxanthin epoxidase (ZE) to reform Viol. The Zea made by the xanthophyll cycle replaces Viol. The *A. thaliana npq*1 mutant, which is inhibited in its ability to convert Viol to Zea shows very little qE,[15] while the mutant *npq*2 which accumulates Zea yet lacks Viol showed unimpaired qE.[11] It was also found that the nearly maximal level (80%) of qE and maximum concentration of Zea was already observed after preillumination at 300 μE $m^{-2}s^{-1}$ of *A. thaliana*.[16]

These results indicate a vital role for Zea in qE, and the femtosecond absorption spectroscopy was interpreted as showing formation of a charge transfer complex from excited Chl and ground-state Zea to form $Chl^{\bullet-}$ and $Zea^{\bullet+}$, which then recombined to the ground state in 200 ps.[12] Although this recombination is fast, other chemical reactions can compete with it, notably deprotonation of $Zea^{\bullet+}$. The time scale for proton transfer is measured in femtoseconds[17−19] when proton

Received: June 28, 2012
Revised: January 15, 2013
Published: January 23, 2013

ACS Publications © 2013 American Chemical Society

dx.doi.org/10.1021/jp306387e | *J. Phys. Chem. B* 2013, 117, 2239−2246

Scheme 1. Illustration of the Xanthophyll Cycle[a]

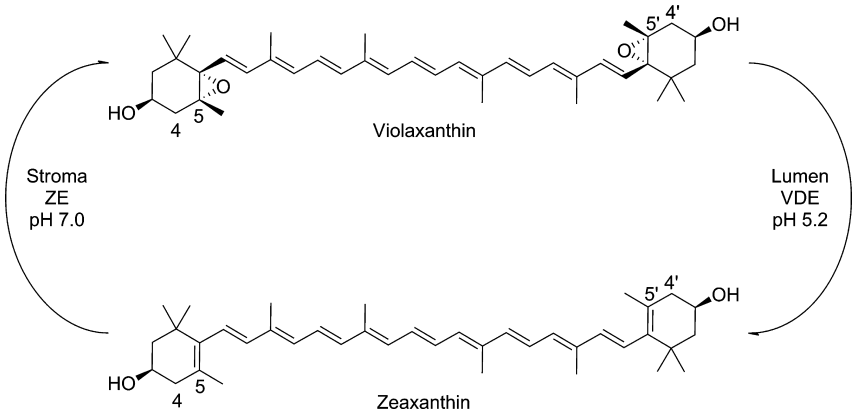

[a]In the presence of as little as room light (4 μE m^{-2} s^{-1}), VDE is triggered by excess protons in the lumen lowering the pH. VDE de-epoxidizes Viol to form Zea. In the absence of light ZE is generated, which epoxidizes Zea to form Viol.

donors and acceptors are preassembled. For instance, proton transfer from an amine to an oxygen takes place with a time constant[20] of 35 fs in photoexcited 2-(2′-hydroxyphenyl)-benzothiazole with the donor/acceptor groups separated by a distance of 2.8 Å.[21] Similarly, proton-coupled electron transfer reactions can be quite fast.[22−24] It is not possible to dismiss the possibility of deprotonation competing with collapse of the charge transfer state.

Our electrochemistry studies show that carotenoid radical cations are weak acids (pK_a 4−7). The most acidic protons are at carbon atoms where their loss results in the largest conjugation length and depends on the donor/acceptor substituents of a carotenoid.[25−27] In the case of $Zea^{\bullet+}$, proton loss occurs from the terminal rings at the C4(4′) methylene or from the methyl groups at the C5(5′) carbon with the C4(4′) being the most favorable.[6] On the other hand, the epoxide groups on the terminal rings of Viol prevent proton loss from the rings, and proton loss occurs only from the methyl protons located in the center of the polyene chain. Proton loss to form neutral radicals occurs in the electrochemical solutions for both Viol and Zea.[6] In the solid state, $\#Zea^{\bullet}$ forms from $Zea^{\bullet+}$ very efficiently, even at 77 K after photo-oxidation[28] of Zea on silica−alumina solid supports at $\lambda \sim 350$ nm. In electrochemical solutions and in the solid supports, all protons on the carotenoid radical cations have similar access to proton acceptors so that deprotonation is determined mainly by the acidity of the radical cation. However, in proteins, this is not the case because the carotenoids are typically in a highly ordered environment, and the long chain is typically embedded in a very nonpolar region, lacking proton acceptors, while the rings are in more polar environments.

The crystal structure of the CP29 minor antenna component (Protein Data Bank 3PL9) where qE was found shows that in one terminal ring, the C4(4′) of Viol XAT662 is in close proximity (<4 Å) to an axial water ligand HOH307 on Chl CLA604 and another water HOH244, which could act as proton acceptors. A network of water molecules lies within hydrogen bonding distance of each other, as well as the hydroxyl at C3(3′) and another oxygen on Chl CLA604. This network suggests that the water plays a functional or structural role in the protein and would remain in place after the Viol XAT662 is replaced by Zea during light stress. Any $Zea^{\bullet+}$ that is formed has proton-accepting groups nearby the acidic C4(4′) positions so that deprotonation is possible. These conditions could allow formation of $\#Zea^{\bullet}$. On the other hand, any $Viol^{\bullet+}$ would be unable to lose protons from the ring, and proton loss from the chain is prevented because no proton acceptors are available in the nonpolar protein region holding the chain.[6,28]

If $\#Zea^{\bullet}$ is formed, what is its relevance to qE? Deprotonation would leave $Chl^{\bullet-}$ and $\#Zea^{\bullet}$ in the protein. Recombination is prevented because deprotonation drastically shifts the redox potential of Zea.[25] The radical ions of Chl undergo facile electron transfer with Chl in photosystem I and II as well as in light harvesting complexes.[29−36] The Chl radical is likely to jump to other Chls in the protein complex to separate the $\#Zea^{\bullet}$ and $Chl^{\bullet-}$ while extending their lifetimes because they would need to come together again and transfer a proton back to Zea to form the charge transfer complex before they could recombine. However, in the time before they recombine, both radicals can encounter many Chl excited states.

Free radicals and other paramagnetic species such as molecular oxygen are generally potent quenchers of excited states by electron exchange-induced-quenching. Quenching by free radicals[37,38] is important in liquids and solids and forms the basis for fluorescence detection of reactive oxygen species. Quenching of fluorescence by J exchange for either an excited single or triplet state has been accomplished by attaching a stable nitroxide neutral radical as far away as 9 Å from a fluorescing molecule. This is demonstrated by Hideg[38] via fluorescence quenching in two reactive oxygen species sensors; singlet oxygen specific DanePy and OH-1889NH, which reacts with both singlet oxygen and superoxide radicals. A similar situation would occur if $\#Zea^{\bullet}$ is near an excited Chl in CP29 or similar proteins. Each $\#Zea^{\bullet}$ would become a potent free radical trap for large numbers of excited Chl, potentially making a major contribution to qE even if its quantum yield is small. Yet, possible impact of $\#Zea^{\bullet}$ in qE seems to have been overlooked.

Approach to Study. We look for evidence of #Zea• formation during qE in the form of H/D exchange in Zea. We infiltrated leaves of wild-type *A. thaliana* with D_2O and examined the relative isotopic distribution of Zea via liquid chromatography/mass spectrometry (LC/MS). If deprotonation of $Zea^{\bullet+}$ occurs, the $\#Zea^{\bullet}$ could reprotonate with a deuterium to $d_1Zea^{\bullet+}$ and subsequently could be reduced to d_1Zea. This would shift the relative distribution of the different isotopic species: Zea, d_1Zea, and d_2Zea. Zea has a molecular

dx.doi.org/10.1021/jp306387e | J. Phys. Chem. B 2013, 117, 2239−2246

mass of 568.9 g/mol, denoted as "M", while d_1Zea and d_2Zea have masses of M+1 and M+2 respectively. Zea has an OH group on each terminal ring that readily exchange with H or D in the solvent. To prevent exchange of OH groups from affecting the mass distributions, all extracted carotenoid samples were equilibrated with protonated solvents before and during LC/MS. This ensured that all OH groups had the natural isotopic abundance and that the mass distribution reflected primarily the H/D distribution of the C−H groups. The theoretical distribution of the M, M+1, and M+2 mass peaks should be approximately 100, 44, and 10 due to the natural abundance of ^{13}C. Zea is readily protonated during electrospray ionization (ESI)[39] forming a mixture of $[Zea+H]^+$ and $[Zea^{\bullet+}]$ ions, which skews our isotopic distribution from the theoretical distribution. To compensate for this, it was important to compare consecutive sets of experiments measured under identical conditions using single factor analysis of variance (ANOVA). This analysis determines whether there are any statistically significant differences in the amount of d_1Zea and d_2Zea between the various samples.

H/D exchange can be caused by processes other than qE, and it is necessary to determine whether non-qE processes are involved. One approach is to use mutants deficient in qE as in the femtosecond absorption measurements. This approach has the major drawback that exposing the mutants to high light levels will cause photochemical damage that is not present in leaves protected by qE, making it problematic to attribute results to qE or photodamage. We therefore used the light level in wild-type *A. thaliana* to modulate qE and other physiological processes that might lead to H/D exchange.

Leaves were infiltrated with either D_2O or H_2O and exposed to varying levels of light intensity; both above and below that needed to induce NPQ in *A. thaliana* (300 μE m^{-2} s^{-1}).[40] Leaves exposed to light intensity less than needed to induce NPQ but high enough to trigger the xanthophyll cycle were measured to determine whether any H/D exchange occurred during interconversion of Zea and Viol in the xanthophyll cycle. Control samples were kept in the dark to check whether other physiological processes or Zea isolation caused H/D exchange. We expected that only a fraction of Zea would undergo H/D exchange since only a fraction of the Zea participates in qE. Avenson et al.[13] demonstrated that a majority of Zea binding proteins do not undergo charge transfer quenching, and thus could not undergo H/D exchange. The amount of H/D exchange is also limited because not all water molecules can be replaced by D_2O. Following infiltration of wild-type *A. thaliana* leaves with D_2O or H_2O and exposure to light intensity less than or greater than that needed to induce NPQ, the carotenoids were extracted and analyzed via LC/MS. The relative mass distribution of Zea was measured to check for formation of $\#Zea^{\bullet}$ during qE.

The ability to form neutral radicals depends on the local environment of the carotenoid in its complex with the protein, the terminal groups, and the presence of nearby proton acceptors. All of these conditions are satisfied by Zea in the CP29 minor antennae component where qE seems to occur. It is not known if they do in the other antenna proteins, CP24 and CP26, that also support $Zea^{\bullet+}$ formation during qE because there is no structure of those complexes in the structural databases. Although we suggested that $\#Zea^{\bullet}$ may be present during qE, based on the known chemistry of $Zea^{\bullet+}$, there has been no experimental evidence of its presence during qE until the H/D exchange measurements reported here.

METHODS AND MATERIALS

Plant Material. Columbia wild-type (Col-0) seeds of *A. thaliana* were planted in 4″ × 4″ × 3.75″ pots (Hummert International) in Pro-Mix HP soil (Premier). Plants were grown under 16/8 h day/night cycles at approximately 23 °C/21 °C, respectively. The average light intensity at the top of the pots was approximately 100 μE m^{-2} s^{-1}. Plants were watered with fertilizer (Petersen's 20−20−20) twice a week or as needed. Leaves were collected from 4 to 5 week old *A. thaliana* plants.

H_2O and D_2O Infiltration of Leaves. *A. thaliana* leaves were placed into a syringe. Distilled water or D_2O was added until the leaves were completely submerged. The syringe needles were plugged into a cork, and the plunger was drawn to create a vacuum that was held for 2 min and then released. This process infiltrated the leaves with either H_2O or D_2O.

Light Exposure. Infiltrated leaves were exposed to light intensity less than needed to induce qE by placing half of the leaves from each syringe outside on a cloudy day for 30 min at approximately 150 μE m^{-2}s^{-1} light intensity. This intensity is sufficient to initiate the xanthophyll cycle, but not qE. These will be referred to as the below qE threshold samples and denoted "BTW" for the water infiltrated and "BTD" for the D_2O infiltrated. The other half of the leaves from each syringe was used as controls (C) and received a sham exposure in a closed styrofoam shipping box. These will be referred to as the below qE threshold controls or "BTW-C" for the water infiltrated control and "BTD-C" for the D_2O infiltrated control.

Infiltrated leaves were exposed to light intensity greater than needed to induce qE by placing half of the leaves from each syringe outside on a sunny day for 30 min at approximately 370 μE m^{-2} s^{-1} light intensity. This intensity is sufficient to initiate both the xanthophyll cycle and qE. These will be referred to as the above qE threshold samples and denoted "ATW" for the water infiltrated and "ATD" for the D_2O infiltrated. The other half of the leaves from each syringe was used as controls (C) and received a sham exposure in a closed styrofoam shipping box. These will be referred to as the above qE threshold controls or "ATW-C" for the water infiltrated control and "ATD-C" for the D_2O infiltrated control.

Carotenoid Extraction. The exposed leaves from the *A. thaliana* plant were placed into Eppendorf tubes and crushed with a tissue homogenizer. A small amount of anhydrous sodium sulfate was added and crushed with the homogenizer again. Then, 0.5 mL of high-performance liquid chromatography (HPLC)-grade acetone was added and vigorously shaken for 30 s. Another 0.5 mL of HPLC-grade acetone was added and shaken again for 30 s. 0.5 mL of this acetone solution was transferred to a new Eppendorf tube while the rest was discarded. HPLC-grade hexane (0.8 mL) was then added to the extracted acetone solution.[41] The tubes were centrifuged until two visible layers formed. The upper green layer was placed into a glass storage vial, while the rest was discarded. The extract was then dried under a stream of N_2 gas and capped. The dried extract was dissolved in 2.5 mL of dichloromethane for LC/MS analysis.

Liquid Chromatography/Mass Spectrometry Analysis. Samples were analyzed using liquid chromatography/mass spectrometry with an Agilent Technologies 1200 series, with an Agilent Technologies Zorbax SB-C18 5 μm 150 × 0.5 mm column. The mass spectrometer was a Bruker HCTultra PTM Discovery system. The flow rate of the chromatography was 18

dx.doi.org/10.1021/jp306387e | J. Phys. Chem. B 2013, 117, 2239−2246

μL/second. The solvent system was an isocratic mixture of 92% methanol diluted with high-purity water (95) and LC/MS grade acetonitrile (5). Both solutions contained 0.1% formic acid by volume. The mass spectrum was generated by using ESI technique in positive ion mode.[42] The chromatograms were analyzed using DataAnalysis version 4.0 (Build 234) from Bruker Daltonic. The chromatograms can be found in the Supporting Information section in Figures S1−S38.

Statistical Evaluation. The data was subject to statistical analysis by one way analysis of variance (ANOVA) using Microsoft Excel 2010 Analysis Toolpak with α set to 0.05. This corresponds to a confidence level of 95%. A p value, the probability that differences between samples are due entirely to random processes, of less than <0.05 was considered statistically significant. The full data sets can be found in the Supporting Information section in Tables S1−S13.

Chemical Formation of Zea Radicals. The radicals were generated via addition of Fe(III)[43] (from $FeCl_3$) dissolved in either water or D_2O equal to 10% molar concentration of the carotenoid solution. Five separate samples were prepared. One sample was left untouched, two samples had Fe(III) added as well as 1% by volume of D_2O (one a few hours prior to LC/MS injection and one 10 min prior), and the other two had Fe(III) added as well as 1% by volume H_2O (one a few hours prior to LC/MS injection and one 10 min prior). These five samples will be referred to as normal, short-term H_2O, long-term H_2O, short-term D_2O, and long-term D_2O. The formation of the radicals was confirmed via optical spectroscopy by the appearance of a peak in the 800−900 nm range.[43]

RESULTS

Confirmation of Zea/Viol Extraction. Both Zea and Viol were present in significant amounts in each extracted plant sample, although the relative amounts vary with light conditions. Their LC/MS peak assignments were confirmed by comparison with purified samples[44,45] used as standards. The extracted ion chromatograms (EICs) at m/z 568.9 of both the Zea standard (Figure 1a) and ATW-C extract (Figure 1b) showed peaks at similar retention times. Similar results were found for the EICs at m/z 601.9 for Viol (Figure 1c,d). Viol has a molecular weight of 600.9 g/mol, but was readily protonated during the ESI process,[39] and the Viol EIC was much better for m/z 601.9.

The chromatograms showed different patterns of multiple peaks for both Zea and Viol. This is due to the *cis*/*trans* isomers of the carotenoids in the extract.[46] The standards were originally produced from the all-*trans* isomer, but it converts into a mixture over time. Also, previous work has demonstrated that radical cations readily form *cis* isomers from the all-*trans* isomer as illustrated in Scheme 2.[47] Due to this chemistry, the H/D exchange should be most noticeable in the *cis* isomers. In the Zea samples, the earliest peak is the *trans* isomer and the later are various *cis* isomers.

Xanthophyll Cycle Activity. Due to its role in producing Zea, an active xanthophyll cycle is essential to the current study. To verify that it is active, we compared the relative mass peak areas of Viol and Zea (V/Z) in the different samples (Figure 2). The V/Z ratio of the BTW sample was 0.51, while the V/Z ratio from the BTW-C was 0.78 (figure not shown). The V/Z ratio of the ATW sample was 0.54, while the V/Z ratio from the ATW-C was 1.27 (figure not shown). Since Viol is de-epoxidized in the xanthophyll cycle, reduction in the relative amount of Viol compared to Zea from the controls to the light exposed samples demonstrates that the xanthophyll cycle is active under the experimental conditions.

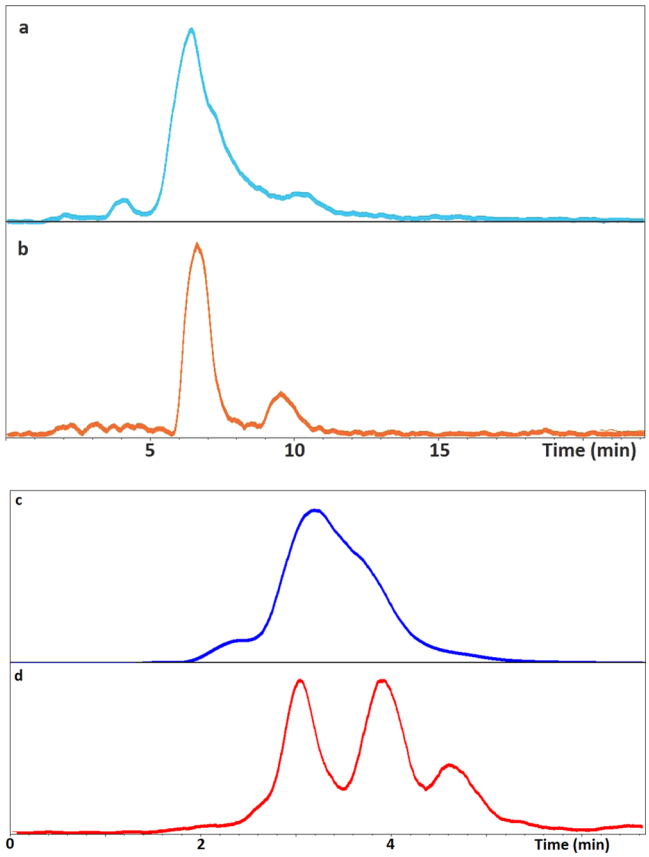

Figure 1. (a,b) EIC at 568.9 m/z of extract from the Zea standard (a) and ATD-C (b). The differences in peak shapes result from the distribution of *cis*/*trans* isomers. (c,d) EIC at 601.9 m/z of Viol standard (c) and ATD-C (d). The differences in peak shapes result from the distribution of the cis/trans isomers.

Chemically-Generated Zea Radicals. The EIC at m/z 568.9 has two distinct peaks (Figure 3) due to *cis*/*trans* isomers as discussed above. The first peak is the all-*trans* isomer, which does not show any significant H/D exchange in the chemically generated radical samples. The second EIC peak is from *cis* isomers.

The average relative intensity of the M+1 peak with mass peak M normalized to 100 for normal and short-term D_2O increased from 55 to 65, which the ANOVA reported $p < 10^{-5}$. This means that there is <0.01% chance the difference is due to random errors in the measurement process and easily meets the usual criterion for statistical significance of $p < 0.05$. The average relative intensity of the M+2 mass peak increased from 14 to 22 ($p < 10^{-6}$) as seen in Figure 4. There is also a statistically significant increase of both the M+1 and M+2 peaks from long-term D_2O compared to normal (both $p = 0.004$).

This isotopic shift could also be seen when comparing the M+1 and M+2 peak intensities from the long-term D_2O samples to the long-term H_2O ones (both $p = 0.001$). Comparing the normal and short-term H_2O samples, the M+1 mass distributions were not statistically different ($p = 0.91$). This experiment demonstrated that H/D exchange readily occurs when Zea radical cations are chemically formed in the presence of D_2O and is detectable via LC/MS. The extent of H/D exchange is probably greater than is indicated here

dx.doi.org/10.1021/jp306387e | J. Phys. Chem. B 2013, 117, 2239−2246

Scheme 2. Possible Routes the Carotenoids Undergo by Electron Transfer to Form Various Isomers

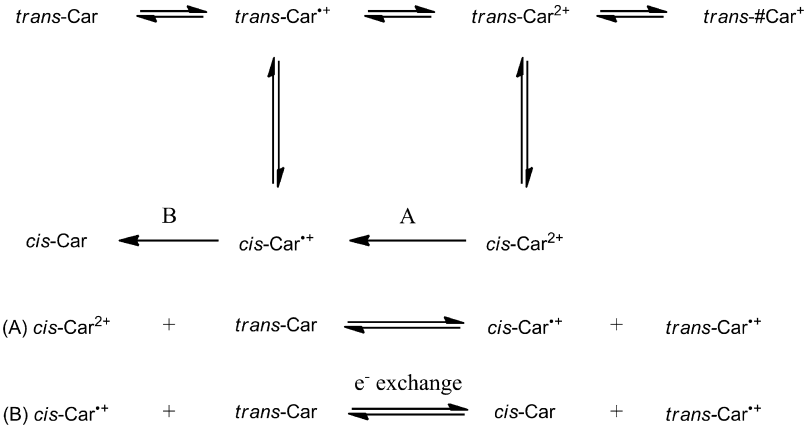

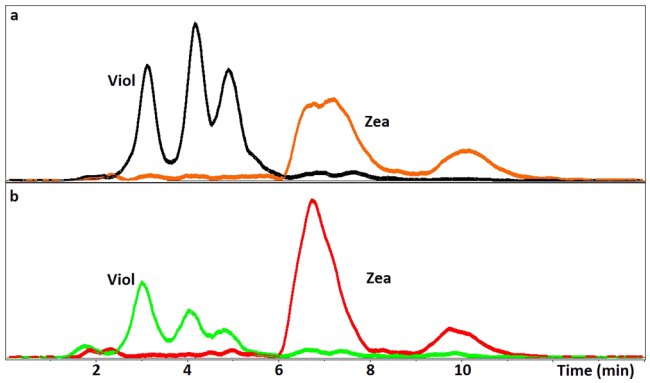

Figure 2. (a,b) EICs from ATW-C (a) and ATW (b). The shifts in the relative intensities from the control samples placed in the box (a) and the samples exposed to light (b) demonstrate xanthophyll cycle activity.

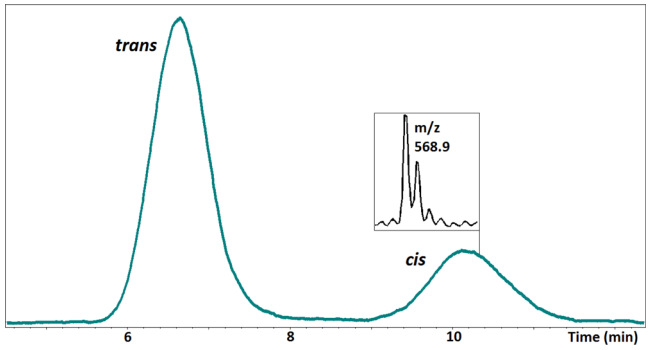

Figure 3. EIC at 568.9 m/z of short-term D_2O Fe(III) added sample with mass spectrum inlay. Two distinct peaks can be seen. The first is from the all-*trans* configuration of Zea. The second is from the *cis* configurations caused by naturally occurring isomers and from the isomerization of Zea during the chemical formation of the radical cations.

because of back exchange when H_2O and methanol are added to the radical cation solutions before preparation for the LC/MS.

Zea H/D Exchange in Leaves. *Below qE-Inducing Light Levels.* Since H/D exchange is detectable via LC/MS for the chemically formed radicals, we now examine the deprotonation of $Zea^{\bullet+}$ during qE. The below qE-inducing light intensity samples showed (Figure 2b) that the xanthophyll cycle was active in these leaves and that there was interconversion between Zea and Viol. Figure 5 shows the relative mass peak intensities of these samples.

The ANOVA for this data found no statistically significant difference in mass distribution for both the M+1 and M+2 data sets (p = 0.20 and 0.60, respectively) between leaves infiltrated with H_2O vs D_2O. There was no difference in mass distribution between any of the sample sets even though the xanthophyll cycle is active in these leaves. These results show that the presence of H_2O or D_2O while the xanthophyll cycle is active and during extraction/measurement causes no detectable difference in isotopic composition of the Zea and indicates that there is no H/D exchange from the xanthophyll cycle or analysis.

Above qE-Inducing Light Samples. The LC/MS mass distributions are shown in Figure 6. Comparison of all the M+1 data sets demonstrated a statistically significant difference ($p < 10^{-3}$) between all the groups. To determine what was causing the variation, more comparisons were done.

Comparisons of the ATW, ATW-C, and ATD-C samples demonstrated no significant statistical differences (p = 0.12–0.63). These results indicate that neither the light exposure by itself nor D_2O infiltration by itself affected the M+1 peak intensity and is consistent with the BTW and BTD results. However, intense light exposure coupled with D_2O infiltration in the ATD samples did produce a statistically significant increase in the M+1 relative peak intensity vs ATW (p = 0.011), ATD-C (p = 0.002), and ATW-C (p = 0.002). Thus, the mass profile indicates H/D exchange only when there is D_2O infiltration coupled with light intensity that induces qE.

The M+2 mass peaks did not show any statistically significant differences. This is understandable from the orientation of Viol observed in the crystal structure, which shows only one terminal ring of Viol (and presumably Zea) in close range to potential proton acceptors. In each ring, the two CH_2 protons at C4(4′) of Zea have different protein environments and are "inequivelant" and may have substantial differences in their ability to be transferred to proton acceptors in the protein complex. The M+2 peaks also are less intense than the M+1 peaks and consequently have relatively more "noise" which could mask real differences. Ahn et al.[12] suggested that charge transfer quenching in CP29 most likely involves two Chl (CLA 602 and CLA609), which are located on the opposite terminal ring from the potential proton acceptors. This suggests that $\#Zea^{\bullet}$ is formed by proton loss on one end of $Zea^{\bullet+}$, while electron transfer to form the initial charge transfer complex

dx.doi.org/10.1021/jp306387e | J. Phys. Chem. B 2013, 117, 2239–2246

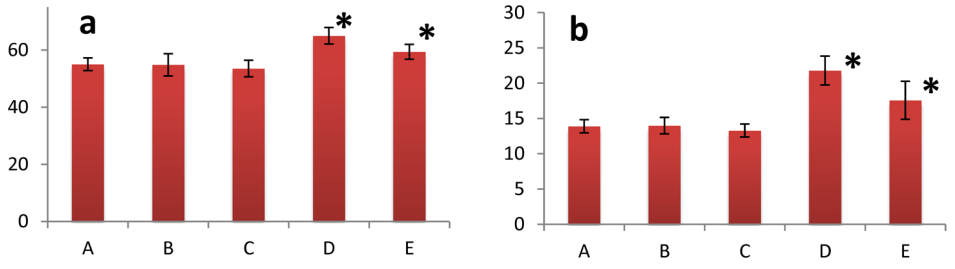

Figure 4. Relative intensities of the M+1 mass peak (a) and M+2 mass peak (b) of the chemically formed *cis* isomer, where *A* = normal, *B* = short-term H_2O, *C* = long-term H_2O, *D* = short-term D_2O, and *E* = long-term D_2O. The D_2O samples showed an increase in relative intensity compared to the normal and H_2O-treated samples. This indicates that H/D exchange is occurring and is detectable via LC/MS. *Denotes statistically significant differences from all other samples ($p < 0.05$).

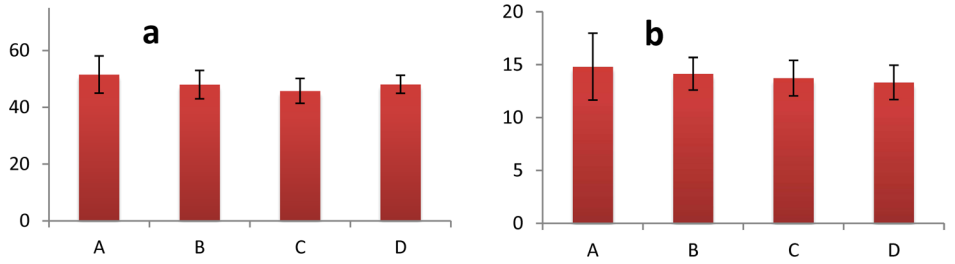

Figure 5. Relative intensities of the M+1 mass peak (a) and M+2 mass peak (b) of the *cis* isomer, with *A* = BTD, *B* = BTW, *C* = BTW-C, and *D* = BTD-C. No statistically significant differences were found when comparing all of the samples.

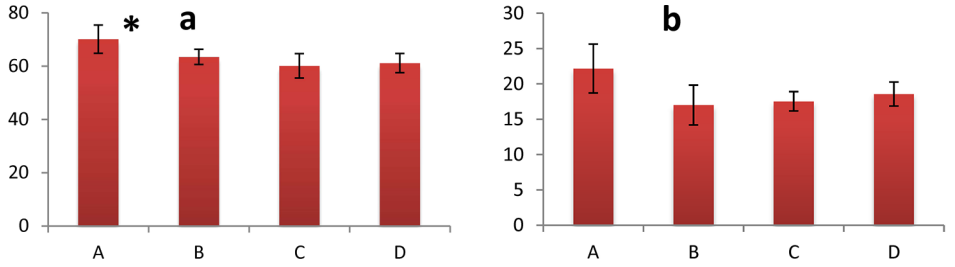

Figure 6. Relative intensities of the M+1 mass peak (a) and M+2 mass peak (b) of the *cis* isomer, with *A* = ATD, *B* = ATW, *C* = ATW-C, and *D* = ATD-C. There is an increase in the size of A in the M+1 mass peak compared to the other samples though not M+2. This is an indication that #Zea$^{\bullet}$ underwent H/D exchange according to the proposed mechanism. *Denotes statistically significant differences from all other samples ($p < 0.05$).

occurs on the other. The extensive delocalization of electrons in Zea allows the protein to carry out electron and proton transfer at different ends of Zea, making it feasible to repeatedly optimize and control these reactions.

Possible Mechanisms for H/D Exchange. Our results show a statistically significant difference in the M+1 mass peak only when D_2O is present during qE. The question that now remains is the origin of the H/D exchange. Could the exchange occur during the conversion of Viol to Zea during the xanthophyll cycle which is active in our samples (Figure 2)? With light intensity less than that needed to induce qE (Figure 5), there are no statistically significant differences in mass distribution for the H_2O and D_2O infiltrated samples. These results show that the xanthophyll cycle by itself cannot be the source of the detected H/D exchange. They also indicate that the *de novo* synthesis of Viol and Zea, and similar metabolic processes, is too slow to have an impact on the isotopic composition of the bulk Zea in the leaves under our experimental conditions.

Figure 6 demonstrates that the only statistically significant difference in the M+1 mass peaks in the leaves occurs for D_2O infiltration with qE-inducing light intensity. These results are consistent with the proposed formation of #Zea$^{\bullet}$ by the deprotonation of Zea$^{\bullet+}$ during qE. We are unaware of other routes to produce isotopically altered Zea that operates only at light intensity above the threshold for qE. There is a need for serious consideration of the role of #Zea$^{\bullet}$ in qE, and for the study of Zea biochemistry in leaves exposed to high light intensity.

CONCLUSION

The formation of #Zea$^{\bullet}$ when a charge-transfer complex Zea$^{\bullet+}$···Chl^{-} is formed between Zea and Chl during qE was examined. Zea$^{\bullet+}$ is acidic (pK_a 4−7) and may deprotonate to form #Zea$^{\bullet}$, which would be a long-lived and efficient quencher of excited state Chl. #Zea$^{\bullet}$ does undergo H/D exchange in the presence of D_2O in solution. We find that leaves from wild-type *A. thaliana* infiltrated with D_2O and exposed to light show H/D exchange in Zea only at light intensity above the threshold needed to induce qE (>300 μE $m^{-2}s^{-1}$). The results are consistent with the formation of #Zea$^{\bullet}$ from Zea$^{\bullet+}$ during qE. The #Zea$^{\bullet}$ is more difficult to reduce than the Zea$^{\bullet+}$ and should have a much longer lifetime in the leaf. The #Zea$^{\bullet}$, like other free radicals, should be a potent quencher of excited state Chl and consequently needs to be considered as an active participant in photoprotection during qE.

dx.doi.org/10.1021/jp306387e | J. Phys. Chem. B 2013, 117, 2239−2246

■ ASSOCIATED CONTENT

Supporting Information

The unsmoothed total ion chromatograms (TICs) are given in Figures S1, S3, S5, S7, S9, S11, S14, S17, S20, S23, S26, S29, S32, S35, and S37. The EICs at m/z 568.9 are given in Figures S2, S4, S6, S8, S10, S12, S15, S18, S21, S24, S27, S30, S33, and S36. The EICs at m/z 601.9 are given in Figures S13, S16, S19, S22, S25, S28, S31, S34, and S38. The data sets that were used in ANOVA comparisons are given in Tables S1–S13. The ANOVA tables are given in Tables S14–S29. This material is available free of charge via the Internet at http://pubs.acs.org.

■ AUTHOR INFORMATION

Notes

The authors declare no competing financial interest.

■ ACKNOWLEDGMENTS

This work was funded by The Chemical Sciences, Geoscience and Biosciences Division, Office of Basic Sciences, U.S. Department of Energy, Grant DE-FG02-86ER-13465 (LDK), that funded a graduate research assistantship for Adam Magyar, support for Lowell Kispert, and supplies for the study; the National Science Foundation CRIF program for the purchase of the ESI/QIT MS, Instrument Grant CHE 0639003 that provided the mass spec data; and the Grant OTKA K-76176 (Hungarian National Research Foundation) to Péter Molnár for isolation of the carotenoid standards. Leaves from the wild type *A. thaliana* were obtained from Dr. Ramonell's research group at The University of Alabama for which we are forever indebted.

■ REFERENCES

(1) Koyama, Y. Structures and Functions of Carotenoids in Photosynthetic Systems. *J. Photochem. Photobiol., B* **1991**, *9*, 265–280.
(2) Renger, G.; Wolff, C. Further Evidence for Dissipative Energy Migration Via Triplet-States in Photosynthesis - Protective Mechanism of Carotenoids in *Rhodopseudomonas spheroides* Chromatophores. *Biochim. Biophys. Acta* **1977**, *460*, 47–57.
(3) Boucher, F.; Vanderrest, M.; Gingras, G. Structure and Function of Carotenoids in Photoreaction Center from *Rhodospirillum rubrum*. *Biochim. Biophys. Acta* **1977**, *461*, 339–357.
(4) Holt, N. E.; Fleming, G. R.; Niyogi, K. K. Toward an Understanding of the Mechanism of Nonphotochemical Quenching in Green Plants. *Biochemistry* **2004**, *43*, 8281–8289.
(5) Pascal, A. A.; Liu, Z. F.; Broess, K.; van Oort, B.; van Amerongen, H.; Wang, C.; Horton, P.; Robert, B.; Chang, W. R.; Ruban, A. Molecular Basis of Photoprotection and Control of Photosynthetic Light-Harvesting. *Nature* **2005**, *436*, 134–137.
(6) Focsan, A. L.; Molnar, P.; Deli, J.; Kispert, L. Structure and Properties of 9′-*cis*-Neoxanthin Carotenoid Radicals by Electron Paramagnetic Resonance Measurements and Density Functional Theory Calculations: Present in LHC II? *J. Phys. Chem. B* **2009**, *113*, 6087–6096.
(7) Mozzo, M.; Dall'Osto, L.; Hienerwadel, R.; Bassi, R.; Croce, R. Photoprotection in the Antenna Complexes of Photosystem II - Role of Individual Xanthophylls in Chlorophyll Triplet Quenching. *J. Biol. Chem.* **2008**, *283*, 6184–6192.
(8) Bautista, J. A.; Tracewell, C. A.; Schlodder, E.; Cunningham, F. X.; Brudvig, G. W.; Diner, B. A. Construction and Characterization of Genetically Modified Synechocystis sp. PCC 6803 Photosystem II Core Complexes Containing Carotenoids with Shorter Pi-Conjugation Than Beta-Carotene. *J. Biol. Chem.* **2005**, *280*, 38839–38850.
(9) Lakshmi, K. V.; Poluektov, O. G.; Reifler, M. J.; Wagner, A. M.; Thurnauer, M. C.; Brudvig, G. W. Pulsed High-Frequency EPR Study on the Location of Carotenoid and Chlorophyll Cation Radicals in Photosystem II. *J. Am. Chem. Soc.* **2003**, *125*, 5005–5014.
(10) Vasil'ev, S.; Brudvig, G. W.; Bruce, D. The X-ray Structure of Photosystem II Reveals a Novel Electron Transport Pathway between P680, Cytochrome B(559) and the Energy-Quenching Cation, Chl_Z^+. *FEBS Lett.* **2003**, *543*, 159–163.
(11) Niyogi, K. K.; Grossman, A. R.; Bjorkman, O. Arabidopsis Mutants Define a Central Role for the Xanthophyll Cycle in the Regulation of Photosynthetic Energy Conversion. *Plant Cell* **1998**, *10*, 1121–1134.
(12) Ahn, T. K.; Avenson, T. J.; Ballottari, M.; Cheng, Y. C.; Niyogi, K. K.; Bassi, R.; Fleming, G. R. Architecture of a Charge-Transfer State Regulating Light Harvesting in a Plant Antenna Protein. *Science* **2008**, *320*, 794–797.
(13) Avenson, T. J.; Ahn, T. K.; Zigmantas, D.; Niyogi, K. K.; Li, Z.; Ballottari, M.; Bassi, R.; Fleming, G. R. Zeaxanthin Radical Cation Formation in Minor Light-Harvesting Complexes of Higher Plant Antenna. *J. Biol. Chem.* **2008**, *283*, 3550–3558.
(14) Muller-Moule, P.; Conklin, P. L.; Niyogi, K. K. Ascorbate Deficiency Can Limit Violaxanthin De-Epoxidase Activity in Vivo. *Plant Physiol.* **2002**, *128*, 970–977.
(15) Havaux, M.; Niyogi, K. K. The Violaxanthin Cycle Protects Plants from Photooxidative Damage by More Than One Mechanism. *Proc. Natl. Acad. Sci. U.S.A.* **1999**, *96*, 8762–8767.
(16) Kalituho, L.; Beran, K. C.; Jahns, P. The Transiently Generated Nonphotochemical Quenching of Excitation Energy in Arabidopsis Leaves Is Modulated by Zeaxanthin. *Plant Physiol.* **2007**, *143*, 1861–1870.
(17) Formosinho, S. J.; Arnaut, L. G. Excited-State Proton-Transfer Reactions 0.2. Intramolecular Reactions. *J. Photochem. Photobiol., A* **1993**, *75*, 21–48.
(18) Kim, C. H.; Park, J.; Seo, J.; Park, S. Y.; Joo, T. Excited State Intramolecular Proton Transfer and Charge Transfer Dynamics of a 2-(2′-Hydroxyphenyl)benzoxazole Derivative in Solution. *J. Phys. Chem. A* **2010**, *114*, 5618–5629.
(19) Kim, C. H.; Joo, T. Coherent Excited State Intramolecular Proton Transfer Probed by Time-Resolved Fluorescence. *Phys. Chem. Chem. Phys.* **2009**, *11*, 10266–10269.
(20) Barbatti, M.; Aquino, A. J. A.; Lischka, H.; Schriever, C.; Lochbrunner, S.; Riedle, E. Ultrafast Internal Conversion Pathway and Mechanism in 2-(2′-Hydroxyphenyl) benzothiazole: A Case Study for Excited-State Intramolecular Proton Transfer Systems. *Phys. Chem. Chem. Phys.* **2009**, *11*, 1406–1415.
(21) Aquino, A. J. A.; Lischka, H.; Hattig, C. Excited-State Intramolecular Proton Transfer: A Survey of TDDFT and RI-CC2 Excited-State Potential Energy Surfaces. *J. Phys. Chem. A* **2005**, *109*, 3201–3208.
(22) Hazra, A.; Soudackov, A. V.; Hammes-Schiffer, S. Role of Solvent Dynamics in Ultrafast Photoinduced Proton-Coupled Electron Transfer Reactions in Solution. *J. Phys. Chem. B* **2010**, *114*, 12319–12332.
(23) Saveant, J. M. Electrochemical Approach to Proton-Coupled Electron Transfers: Recent Advances. *Energy Environ. Sci.* **2012**, *5*, 7718–7731.
(24) Weinberg, D. R.; Gagliardi, C. J.; Hull, J. F.; Murphy, C. F.; Kent, C. A.; Westlake, B. C.; Paul, A.; Ess, D. H.; McCafferty, D. G.; Meyer, T. J. Proton-Coupled Electron Transfer. *Chem. Rev.* **2012**, *112*, 4016–4093.
(25) Liu, D. Z.; Gao, Y. L.; Kispert, L. D. Electrochemical Properties of Natural Carotenoids. *J. Electroanal. Chem.* **2000**, *488*, 140–150.
(26) Liu, D.; Kispert, L. Electrochemical Aspects of Carotenoids. *Recent Res. Dev. Electrochem.* **1999**, *2*, 139–157.
(27) Khaled, M.; Hadjipetrou, A.; Kispert, L. D. Simultaneous Electrochemical and Electron-Paramagnetic Resonance Studies of Carotenoid Cation Radicals and Dications. *J. Phys. Chem.* **1991**, *95*, 2438–2442.
(28) Focsan, A. L.; Bowman, M. K.; Konovalova, T. A.; Molnar, P.; Deli, J.; Dixon, D. A.; Kispert, L. D. Pulsed EPR and DFT Characterization of Radicals Produced by Photo-oxidation of

Zeaxanthin and Violaxanthin on Silica-Alumina. *J. Phys. Chem. B* **2008**, *112*, 1806−1819.
(29) Hasjim, P. L.; Lendzian, F.; Ponomarenko, N.; Norris, J. R. Basic Molecular Unit Involved in Charge Migration in Oxidized Light-Harvesting Complex 1 of *Rhodobacter sphaeroides*. *J. Phys. Chem. Lett.* **2010**, *1*, 1687−1689.
(30) Hasjim, P. L.; Lendzian, F.; Ponomarenko, N.; Weber, S.; Norris, J. R. ENDOR Study of Charge Migration in Photosynthetic Arrays of *Rhodobacter sphaeroides*. *ChemPhysChem* **2010**, *11*, 1258−1264.
(31) Srivatsan, N.; Kolbasov, D.; Ponomarenko, N.; Weber, S.; Ostafin, A. E.; Norris, J. R. Cryogenic Charge Transport in Oxidized Purple Bacterial Light-Harvesting 1 Complexes. *J. Phys. Chem. B* **2003**, *107*, 7867−7876.
(32) Srivatsan, N.; Weber, S.; Kolbasov, D.; Norris, J. R. Exploring Charge Migration in Light-Harvesting Complexes Using Electron Paramagnetic Resonance Line Narrowing. *J. Phys. Chem. B* **2003**, *107*, 2127−2138.
(33) Kolbasoy, D.; Srivatsan, N.; Ponomarenko, N.; Jager, M.; Norris, J. R. Modeling Charge Transfer in Oxidized Bacterial Antenna Complexes. *J. Phys. Chem. B* **2003**, *107*, 2386−2393.
(34) Ostafin, A. E.; Ponomarenko, N. S.; Popova, J. A.; Jager, M.; Bylina, E. J.; Norris, J. R. Characterization of Expressed Pigmented Core Light Harvesting Complex (LH 1) in a Reaction Center Deficient Mutant of *Blastochloris viridis*. *Photosynth. Res.* **2003**, *77*, 53−68.
(35) Srivatsan, N.; Norris, J. R. Electron Paramagnetic Resonance Study of Oxidized B820 Complexes. *J. Phys. Chem. B* **2001**, *105*, 12391−12398.
(36) Norris, J. R.; Scheer, H.; Katz, J. J. Models for Antenna and Reaction Center Chlorophylls. *Ann. N.Y. Acad. Sci.* **1975**, *244*, 260−280.
(37) Green, J. A.; Singer, L. A.; Parks, J. H. Fluorescence Quenching by Stable Free-Radical Di-*tert*-butylnitroxide. *J. Chem. Phys.* **1973**, *58*, 2690−2695.
(38) Hideg, E.; Barta, C.; Kalai, T.; Vass, I.; Hideg, K.; Asada, K. Detection of Singlet Oxygen and Superoxide with Fluorescent Sensors in Leaves under Stress by Photoinhibition or UV Radiation. *Plant Cell Physiol.* **2002**, *43*, 1154−1164.
(39) Guaratini, T.; Vessecchi, R.; Pinto, E.; Colepicolo, P.; Lopes, N. P. Balance of Xanthophylls Molecular and Protonated Molecular Ions in Electrospray Ionization. *J. Mass. Spectrom.* **2005**, *40*, 963−968.
(40) Shikanai, T.; Munekage, Y.; Shimizu, K.; Endo, T.; Hashimoto, T. Identification and Characterization of Arabidopsis Mutants with Reduced Quenching of Chlorophyll Fluorescence. *Plant Cell Physiol.* **1999**, *40*, 1134−1142.
(41) Lakshminarayana, R.; Raju, M.; Krishnakantha, T. P.; Baskaran, V. Determination of Major Carotenoids in a Few Indian Leafy Vegetables by High-Performance Liquid Chromatography. *J. Agric. Food Chem.* **2005**, *53*, 2838−2842.
(42) Van Breemen, R. B. Liquid Chromatography/Mass Spectrometry of Carotenoids. *Pure Appl. Chem.* **1997**, *69*, 2061−2066.
(43) Gao, Y. L.; Kispert, L. D. Reaction of Carotenoids and Ferric Chloride: Equilibria, Isomerization, and Products. *J. Phys. Chem. B* **2003**, *107*, 5333−5338.
(44) Molnar, P.; Szabolcs, J.; Radics, L. Naturally-Occurring Di-*cis*-violaxanthins from Viola-Tricolor - Isolation and Identification by ^{1}H NMR Spectroscopy of 4 Di-*cis*-isomers. *Phytochemistry* **1986**, *25*, 195−199.
(45) Molnar, P.; Szabolcs, J. Occurrence of 15-*cis*-Violaxanthin in Viola-Tricolor. *Phytochemistry* **1980**, *19*, 623−627.
(46) Jeevarajan, A. S.; Wei, C. C.; Kispert, L. D. Geometrical Isomerization of Carotenoids in Dichloromethane. *J. Chem. Soc., Perkins Trans. 2* **1994**, *4*, 861−869.
(47) Gao, G.; Wei, C. C.; Jeevarajan, A. S.; Kispert, L. D. Geometrical Isomerization of Carotenoids Mediated by Cation Radical Dication Formation. *J. Phys. Chem.* **1996**, *100*, 5362−5366.